Research Paper

GEOSPHERE

GEOSPHERE; v. 15, no. 1

https://doi.org/10.1130/GES02015.1

8 figures; 1 set of supplemental files

CORRESPONDENCE: scjohnst@calpoly.edu

CITATION: Johnston, S.M., Singleton, J.S., Chapman, A.D., and Murray, G., 2018, Geologic map and structural development of the northernmost Sur Nacimiento fault zone, central California coast: Geosphere, v. 15, no. 1, https://doi.org/10.1130/GES02015.1.

Science Editor: Shanaka de Silva
Associate Editor: Terry L. Pavlis

Received 30 May 2018
Revision received 19 September 2018
Accepted 7 November 2018

Geologic map and structural development of the northernmost Sur-Nacimiento fault zone, central California coast

Scott M. Johnston[1], John S. Singleton[2], Alan D. Chapman[3], and Gabriella Murray[1]

[1]Physics Department, California Polytechnic State University, San Luis Obispo, California 93407, USA
[2]Department of Geosciences, Colorado State University, Fort Collins, Colorado 80523, USA
[3]Geology Department, Macalester College, St. Paul, Minnesota 55105, USA

ABSTRACT

The Sur-Nacimiento fault exposed along the central California coast (United States) juxtaposes the Salinian block arc against the Nacimiento block accretionary complex, cuts out the majority of the forearc basin and western arc, and requires a minimum of 150 km of orogen-normal crustal excision within the Mesozoic California convergent margin. Despite this significant strain, the kinematic evolution of the Sur-Nacimiento fault remains poorly understood, with diverse hypotheses suggesting sinistral, dextral, thrust, or normal displacement along the fault. This Late Cretaceous–Paleogene strain history is complicated by the location of the fault within a belt of subparallel faults that have accommodated significant Oligocene and younger dextral displacement between the Pacific and North American plates. In the vicinity of Big Creek along the Big Sur coast, steeply bounded bedrock enclaves of Salinian block affinity are enclosed within Nacimiento block mélange, and have been used to support multiple kinematic models for Late Cretaceous–Eocene Sur-Nacimiento slip.

The work presented here targets coastal outcrops from McWay Falls to Gamboa Point, where our new mapping documents Salinian enclaves within Franciscan mélange along several steeply NE-dipping strands of the fault. Between these strands, bedding-parallel gouge zones as much as 2 m wide dip 50°–70°NE and display P-Y fabrics and asymmetric blocks indicating dextral displacement. Kinematic analysis of 401 individual outcrop-scale brittle faults and Y-plane surfaces record dominantly NW-SE extension and NE-SW shortening oblique to the strike of the Sur-Nacimiento fault. At McWay Falls, shear-sense indicators in mylonitic calcite marble found along the McWay fault yield top-South thrust displacement of Salinian basement over Salinian sedimentary rocks. South of the McWay fault, Salinian sedimentary rocks are overturned adjacent to and within strands of the Sur-Nacimiento fault, and display a subvertical E-W–striking disjunctive cleavage. These results are consistent with pre-Miocene N-S shortening or dextral transpression adjacent to the Sur-Nacimiento fault, followed by 8–11 km of Neogene dextral slip along the Gamboa fault that reactivated preexisting NW-SE–striking structures along this segment of the Sur-Nacimiento fault. This study highlights the multiple episodes of deformation along the Sur-Nacimiento fault that obscure the fault's early slip evolution with respect to the juxtaposition of the Salinian and Nacimiento blocks, as well as the potential that dextral reactivation of the Sur-Nacimiento fault may partially accommodate differential displacement along the San Gregorio–Hosgri fault.

INTRODUCTION

Accretionary complex–forearc basin–magmatic arc triads preserved in ancient and modern convergent margins are commonly characterized by syn- to post-orogenic deformation that is localized within the forearc by rheological contrasts between arc and forearc domains (e.g., Pavlis and Roeske, 2007). This deformation obscures our understanding of convergent margin processes associated with the removal of forearc domains, including regional contraction (e.g., Grove et al., 2008; Keppie et al., 2012), tectonic erosion (e.g., von Huene and Scholl, 1991; Clift and Vannucchi, 2004), slip-partitioned transpression (e.g., McCaffrey et al., 2000; Wyld et al., 2006), and lateral escape due to collision of a rigid indenter (e.g., Tapponnier et al., 1982; Jacobson et al., 2011), as well as how these inherited forearc structures localize strain in subsequent tectonic regimes. Resolution of these processes is commonly complicated by along-strike variability and multiple episodes of deformation that have eliminated regional strain markers between the original convergent margin domains (e.g., Pavlis and Roeske, 2007). However, the Cenozoic transition of the southwestern North American margin from a convergent to a dextral transform plate boundary offers a unique opportunity to study forearc deformation structures and their subsequent reactivation, given that an archetypical example of a convergent margin preserved north of the San Andreas fault (e.g., Dickinson, 2008; Ernst et al., 2008) may be used as a basis for comparison with more deformed segments of the margin farther south.

South of the San Andreas fault and along the central California coast, the omission of the majority of the forearc basin strata and the juxtaposition of Nacimiento block subduction complex and Salinian block arc rocks across the enigmatic Sur-Nacimiento fault (Dickinson, 1983; Hall, 1991; Hall and Saleeby, 2013; Jacobson et al., 2011; Page, 1972, 1970) serve as a reminder of the complexity of forearc deformation in convergent margins. Similarly, along-strike

discrepancies in displacement along the dextral San Gregorio–San Simeon–Hosgri fault north and south of its intersection with the Sur-Nacimiento fault (Lettis et al., 2004; Dickinson et al., 2005; Langenheim et al., 2013; Colgan and Stanley, 2016) highlight the significance of inherited structures in the context of how strain is partitioned between discrete faults and broad deformation zones across the Pacific–North American plate boundary. Characterizing the style of deformation along faults in these archetypical examples from the central California coast is thus central to our understanding of convergent margin and transform margin tectonic settings, and will help identify patterns of tectonic inheritance within ancient forearc assemblages, with implications for hazard assessment worldwide.

To place new constraints on the cumulative strain evolution of the Sur-Nacimiento fault, this study targets the northernmost extent of the Sur-Nacimiento fault along the Big Sur coast from McWay Falls to Gamboa Point, and immediately south of its projected offshore intersection with the San Gregorio–San Simeon–Hosgri fault (Fig. 1). This work builds on previous mapping efforts in the area (Reiche, 1937; Gilbert, 1971; Ross, 1976; Seiders et al., 1983; Norris, 1985; Hall, 1991; Willis et al., 2001; Dibblee and Minch, 2007a, 2007b) by adding detailed mapping of superior exposures in beach outcrops and fault kinematic data from shear zones and late brittle fault surfaces. Our results are consistent with the interpretation that the original structural relationships between the Nacimiento and Salinian blocks across the Sur-Nacimiento fault have been disrupted by two discrete episodes of deformation most likely associated with pre-Miocene dextral-oblique subduction of the Farallon plate and Neogene Pacific–North American plate transform tectonism.

GEOLOGIC SETTING

The California Mesozoic convergent margin assemblage southwest of the San Andreas fault is dissected by the Sur-Nacimiento fault, which juxtaposes Salinian block arc rocks with Nacimiento block subduction complex rocks (e.g., Page, 1970; Fig. 1). The Salinian block consists of Cretaceous magmatic rocks and its metamorphic framework, which are correlated with the southern extension of the Sierran arc (Kistler and Peterman, 1978; Dickinson, 1983) and that are unconformably overlain by upper Cretaceous inner forearc basin strata (Vedder et al., 1983; Grove, 1993). The Nacimiento block consists of Franciscan Complex mélange and broken formation tectonically overlain by remnants of Jurassic ophiolite and forearc basin sedimentary rocks, and is correlative with the Franciscan Complex–Great Valley Group pair exposed along the western margin of the San Joaquin Valley (Gilbert and Dickinson, 1970; Vedder et al., 1983). Cross-cutting relationships and stratigraphic cover constrain the juxtaposition of the Salinan and Nacimiento blocks to ca. 75–60 Ma (Mattinson, 1990; Hall, 1991; Kidder et al., 2003; Dickinson et al., 2005; Jacobson et al., 2011). By analogy with the well-preserved convergent margin tectonic assemblages currently exposed northeast of the San Andreas fault, the omission of the majority of the Mesozoic forearc basin and the western arc requires a minimum of 150 km of orogen-normal crustal excision across the Sur-Nacimiento fault (Fig. 1).

Despite this significant offset along the fault, the slip history of the Sur-Nacimiento fault is poorly understood, and a variety of models have been proposed to explain its kinematic evolution. Dip-slip models suggest that the Nacimiento block originated outboard of the Salinian arc, and that the forearc was thrust beneath the arc along the Sur-Nacimiento fault (Hall, 1991; Johnston et al., 2018), which may have behaved as a normal fault during Late Cretaceous extensional collapse of the southern California arc (Chapman et al., 2016). Sinistral-slip models suggest that the Nacimiento block originated at the modern-day latitude of San Francisco (Seiders, 1983; Dickinson, 1983; Jacobson et al., 2011) or the southern San Joaquin Valley (Johnston et al., 2018), and slipped obliquely across the forearc basin along the Sur-Nacimiento fault and southeastward into contact with the Salinian arc. Alternatively, models that originally place the Nacimiento block at distant equatorial latitudes suggest removal of the forearc basin during allochthonous arrival of the Salinian and Nacimiento blocks in southern California via margin-parallel dextral slip along the Sur-Nacimiento and related faults (McWilliams and Howell, 1982; Page, 1982).

Displacement along the Sur-Nacimiento fault is complicated by Oligocene and younger Pacific–North American plate dextral transform strain. Although dextral slip along the San Andreas fault accommodates the majority of this interplate strain, the sum of Pacific–North American plate strain is distributed across structures found from coastal to eastern California (e.g., Bennett et al., 2003; Titus et al., 2011). Southwest of the San Andreas fault, the San Gregorio–San Simeon–Hosgri fault represents a significant part of this broader transform plate boundary system, with estimates for cumulative dextral slip of 160–125 km along its northern segments (Clark et al., 1984; Dickinson et al., 2005; Langenheim et al., 2013), although slip estimates decrease along its southern segment south of its intersection with the Sur-Nacimiento fault and diminish to zero at its southern terminus adjacent to the Transverse Ranges (Sorlien et al., 1999; Langenheim et al., 2013). Models used to explain the observed southern decrease in San Gregorio–San Simeon–Hosgri fault slip alternately describe large-magnitude NW-SE shortening of the Santa Maria Basin (Dickinson et al., 2005) or shortening and/or dextral displacement across NW-SE–striking faults distributed throughout the Nacimiento block (McLaren and Savage, 2001; Lettis et al., 2004; Hardebeck, 2010; Colgan and Stanley, 2016).

This study investigates exposures of the Sur-Nacimiento fault along the Big Sur coast from McWay Falls to Gamboa Point near its mapped intersection with the San Gregorio–San Simeon–Hosgri fault (Figs. 1, 2). Previous mapping efforts in the region have identified several bedrock enclaves of Salinian block affinity that are fully enclosed within Nacimiento block Franciscan Complex (Reiche, 1937; Gilbert, 1971; Ross, 1976; Seiders et al., 1983; Norris, 1985; Hall, 1991; Willis et al., 2001; Dibblee and Minch, 2007a, 2007b) and which indicate structural repetition of the Sur-Nacimiento fault in this area (Fig. 2). Along this stretch of the fault, the Salinian block consists of Salinian arc basement overlain by Maastrichtian Big Creek conglomerate strata. Salinian block basement rocks consist of Cretaceous plutonic rocks, their metamorphic equivalents,

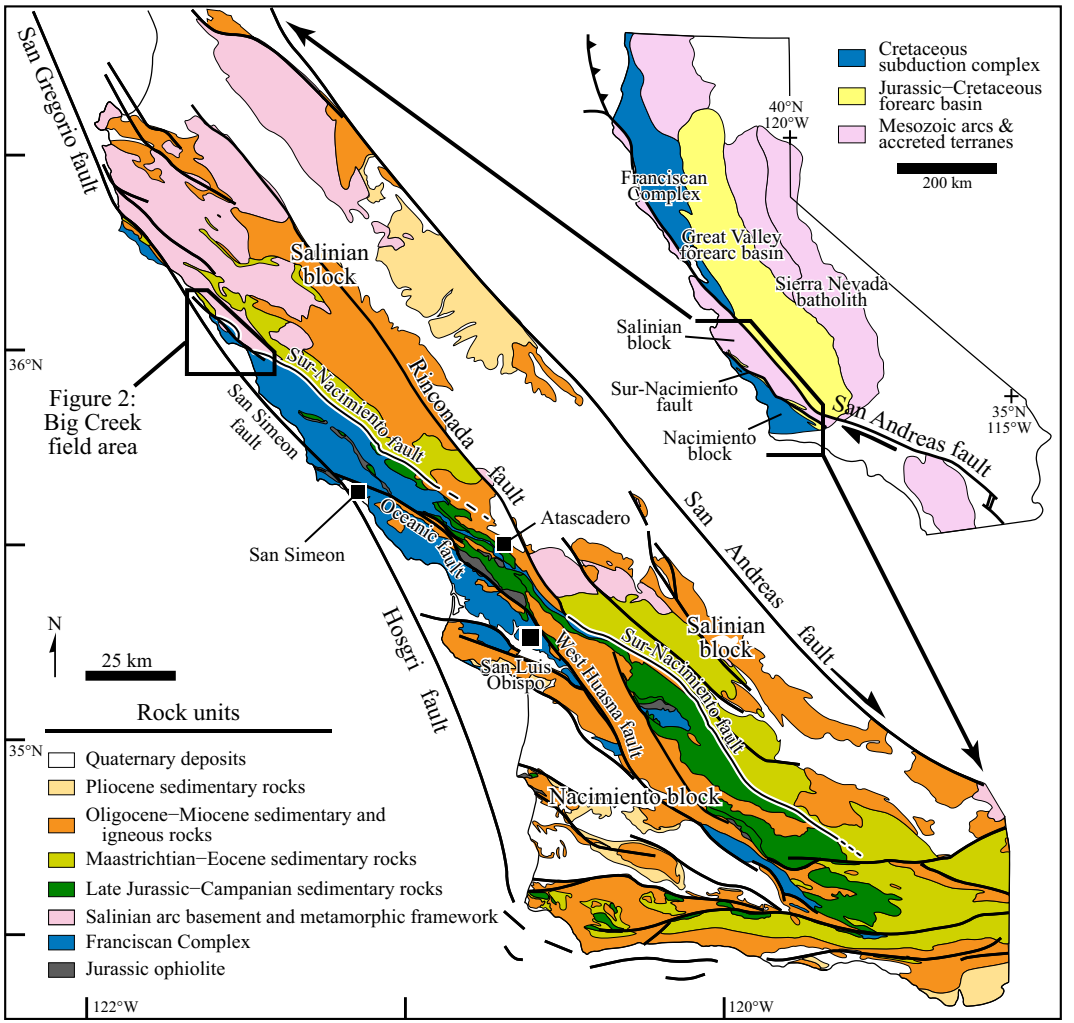

Figure 1. Regional geologic map of the central California coast (western United States) illustrating the location of the field area with respect to tectonic boundaries and faults. Inset illustrates the Mesozoic convergent margin assemblage in northern California and its reorganization by the Sur-Nacimiento and San Andreas faults in southern and central California, respectively. The Sur-Nacimiento fault is dashed where buried or inferred.

and diverse high-grade metamorphic supracrustal rocks that are cumulatively thought to represent exposures of arc lower crust (Compton, 1960; Mattinson, 1978; Hansen and Stuk, 1993; Kidder et al., 2003; Chapman et al., 2014). The Big Creek conglomerate includes ~100 m of boulder-cobble conglomerate with interlayers of coarse sandstone that grade upward into at least another 100 m of stratigraphic section composed of massive sandstone layers 10–200 cm thick that are interlayered with siltstones and shales (Norris, 1985). Big Creek conglomerate strata are interpreted to represent deposition in a submarine canyon and fan system that formed in a shallow- to deep-water basin that was located within, or proximally to, exhumed Salinian block basement (Ruetz, 1979; Norris, 1985). Southwest of the Sur-Nacimiento fault, Nacimiento block basement exposed in the study area is Franciscan Complex mélange composed of a variety of relatively resistant blocks included within a mudstone matrix that is interpreted to have formed within a subduction complex (e.g., Ernst, 1970, 1984; Cowan, 1978; Ukar, 2012; Chapman et al., 2016).

Despite generally consistent map patterns in the existing geologic maps, interpretations of the Salinian enclaves with respect to the geometry of the Sur-Nacimiento fault vary widely. Hall (1991) interpreted the Salinian enclaves

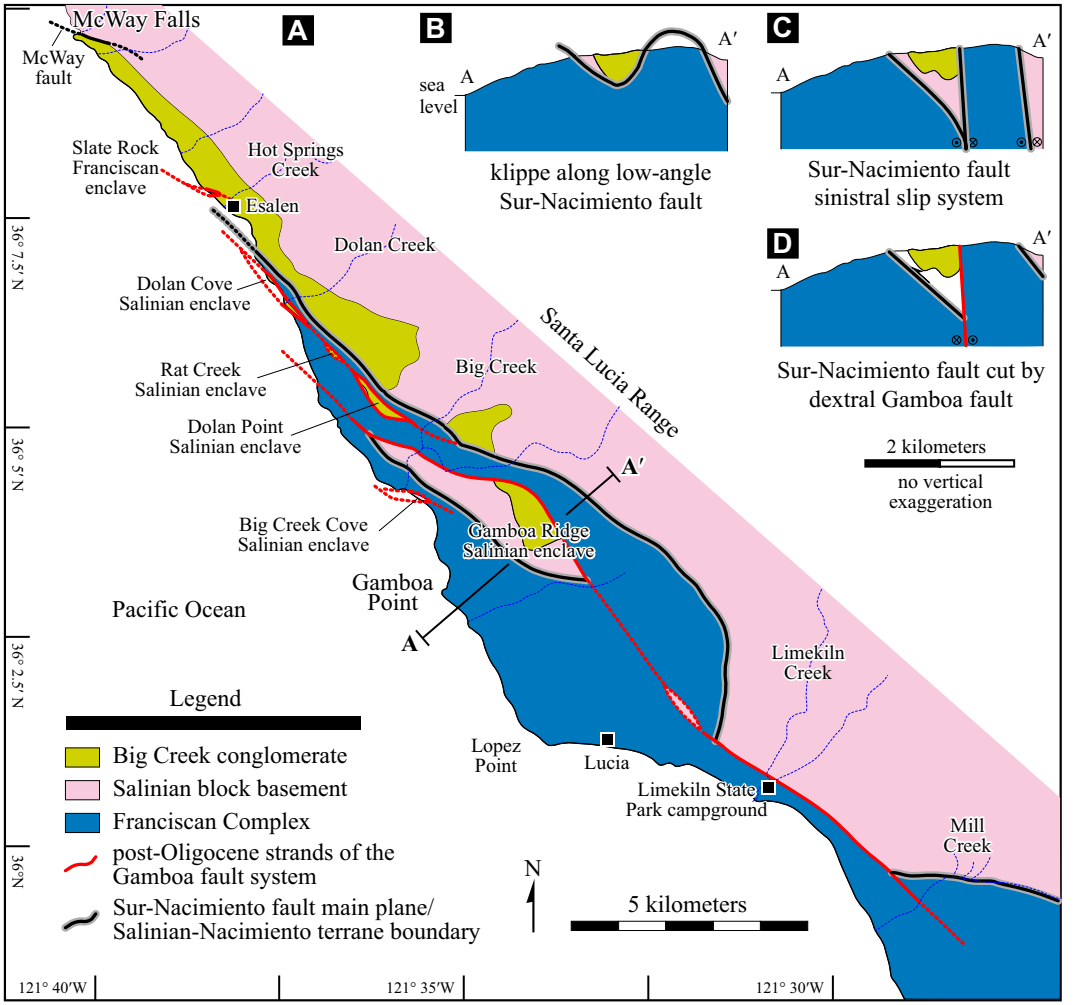

Figure 2. (A) Geologic map of the Big Sur coast from McWay Falls to Mill Creek, illustrating the relative locations of Salinian enclaves with respect to strands of the Sur-Nacimiento and Gamboa faults. Section line A–A′ refers to interpretive cross sections (B–D) that illustrate different fault models. (B–D) Fault models explaining the formation of the Salinian enclaves: low-angle fault after Hall (1991) (B), a high-angle fault system with a sinistral-slip flower structure as suggested by Dickinson et al. (2005) (C), and a high-angle dextral fault that cuts an older low-angle Sur-Nacimiento fault as suggested by Norris (1985) (D).

as erosional remnants of Salinian basement preserved as fault klippe in the hanging wall of a folded low-angle fault (Fig. 2B) associated with top-to-the-southwest, Late Cretaceous–Paleocene thrust displacement of the Salinian arc over the forearc. Chapman et al. (2016) suggested that this potentially low-angle geometry at Big Creek was formed during Late Cretaceous–Paleocene top-to-the-northeast, normal-sense displacement along the fault associated with extensional collapse of Salinian arc. Alternatively, Dickinson et al. (2005) asserted that the steeply dipping contacts that bound the Salinian enclaves are more consistent with strike-slip faulting, and suggested that the enclave geometry was formed as the result of Late Cretaceous–Paleocene sinistral slip along the fault and/or more recent duplication of the originally sinistral structure via kilometer-scale displacement along dextral strands of nearby San Gregorio–San Simeon–Hosgri fault (Figs. 2C, 2D). The study presented here aims to resolve the discrepancies between these models by placing tighter constraints on the geometry and strain history of the multiple strands of the Sur-Nacimiento fault between McWay Falls and Gamboa Point, through detailed mapping of contact relationships and kinematic analysis of outcrop-scale structures found in superbly exposed beach outcrops.

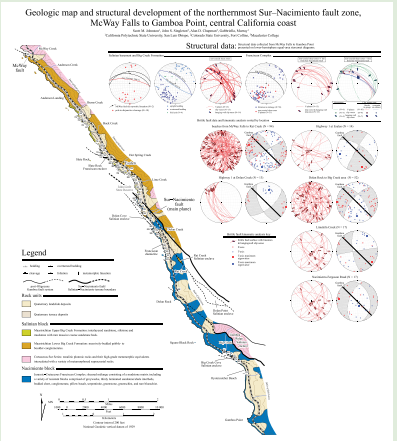

[1]Supplemental Materials. Plate S1: A 1:24,000-scale geologic map of coastal exposures from McWay Falls to Gamboa Point. Table S1: Structural data (Fig. 3) complete with locations and relevant field observations. Please visit https://doi.org/10.1130/GES02015.S1 or access the full-text article on www.gsapubs.org to view the Supplemental Materials.

STRUCTURAL GEOLOGY OF THE BIG SUR COAST FROM MCWAY FALLS TO GAMBOA POINT

The Sur-Nacimiento fault intersects the coastline in several distinct strands between McWay Falls and Gamboa Point, and divides the field area into a northern segment dominantly composed of Salinian-affinity Big Creek conglomerate and a southern segment dominantly composed of Nacimiento-affinity Franciscan Complex (Fig. 2). In the following sections, we describe outcrop-scale structures from rock units adjacent to the fault, followed by a description of the regional geometry of the Sur-Nacimiento fault and its multiple fault strands. A 1:24,000-scale geologic map of coastal exposures from McWay Falls to Gamboa Point is available as Plate S1 in the Supplemental Materials[1]. All structural data (Fig. 3), complete with locations and relevant field observations, are available in Table S1 (footnote 1).

The McWay Fault and Outcrop-Scale Structure of the Big Creek Conglomerate

The McWay fault is best exposed at the northernmost edge of the field area on the rocky peninsula west of McWay Falls, where Salinian garnet-biotite gneiss lies structurally above lower Big Creek conglomerate. Here, the McWay fault is expressed as a shear zone that is several meters thick consist-

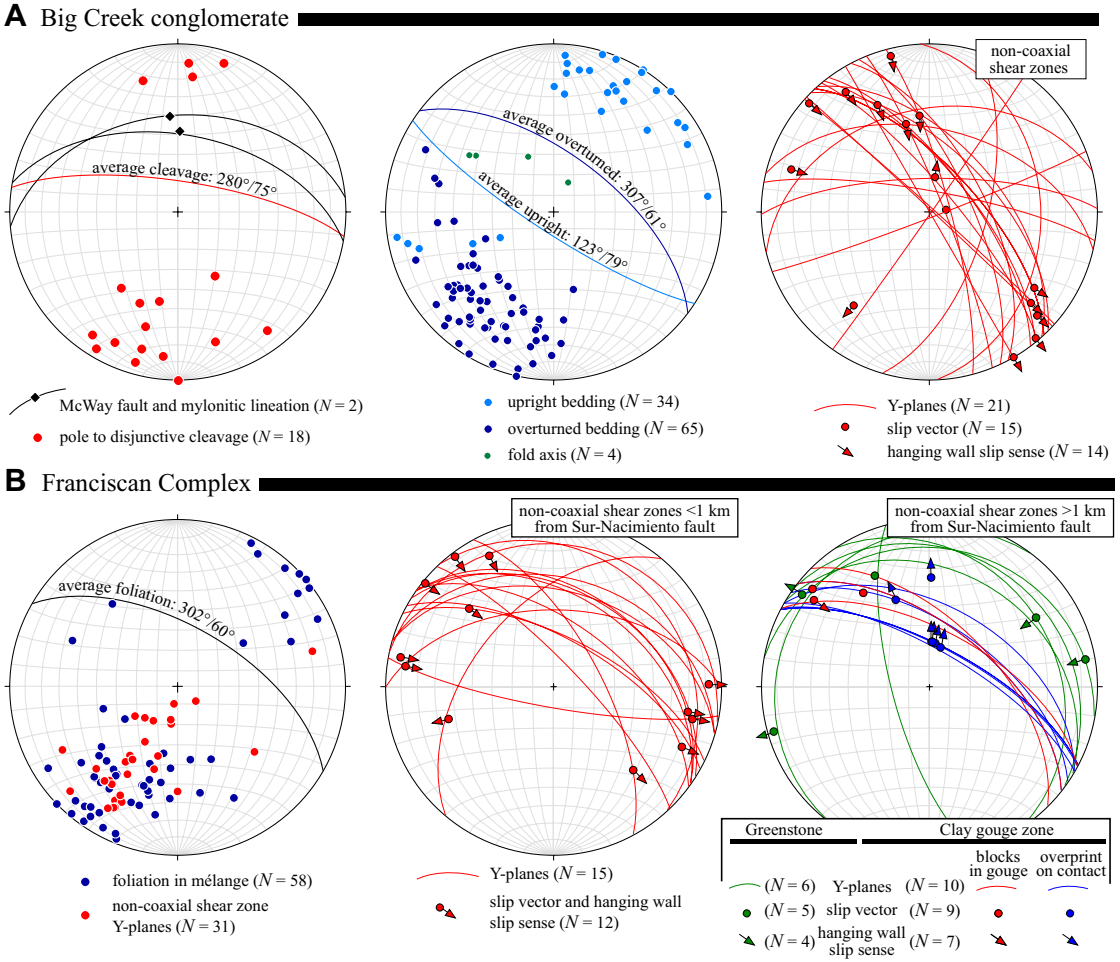

Figure 3. Structural data from McWay Falls to Mill Creek measured in Salinian block basement and Big Creek conglomerate (A) and in Nacimiento block Franciscan Complex (B). Plots are lower-hemisphere, equal-area stereonet diagrams. Notation for average plane orientations refers to strike azimuth°/dip plunge°.

ing of intercalated graphite-rich marble mylonite, chloritized and brecciated tonalite, and black, silicified fault gouges (Fig. 4A). The shear zone is curviplanar, although it generally dips shallowly to the north and displays consistently N-trending, down-dip lineations that are best observed in graphite-rich layers in the marble mylonite. Thin sections of marble mylonites reveal elongate calcite porphyroclasts in low-strain zones that display dominantly type II twins with local examples of type IV twins characterized by recrystallized twin planes. Foliation in these marble mylonites is defined by higher-strain seams characterized by dynamically recrystallized calcite with a mean grain size of 6–7 μm (Fig. 4B). Shear-sense indicators associated with high-strain seams include S-C fabrics, sigma clasts, C′ shear bands, and brittlely attenuated muscovite, and indicate top-to-the-south, thrust-sense slip (Fig. 4B) that is consistent with the observed Salinian arc basement–over–Big Creek conglomerate field relationship. The recrystallized carbonate matrix also includes porphyroclasts of muscovite mica, feldspar, and titanite that we interpret as evidence of mechanical mixing with adjacent Salinian tonalite during fault slip. Farther to the east on the McWay Falls overlook trails and on hillslopes east of State Route 1, the McWay fault is concealed by dense vegetation and Quaternary terrace deposits, and the fault was not identified elsewhere in the current study.

South of McWay Falls, lower Big Creek conglomerate was observed on hillslopes east of Highway 1, where they have been mapped extensively in previous studies (Hall, 1991; Dibblee and Minch, 2007a, 2007b), although coastal exposures south of Burns Creek to the Sur-Nacimiento fault are primarily composed of upper Big Creek conglomerate interlayered sandstone and mudstone. Bedding in this package of upper Big Creek conglomerate dips steeply NE or SW (Fig. 3A) and displays facing indicators indicating that NE-dipping beds are overturned (Fig. 5A). Finer-grained mudstone and siltstone interlayers are commonly characterized by a variably developed disjunctive cleavage that strikes WNW-ESE with subvertical dips (Figs. 3A, 5B). Several outcrop-scale, tight to isoclinal folds with NE-trending, moderately plunging fold axes were observed throughout the field area; in several locations, the disjunctive cleavage is axial planar with respect to the outcrop-scale folds (Figs. 3A, 5C). In thin section, this disjunctive cleavage displays aligned detrital micas and pressure-solution seams within cleavage domains (Fig. 5D). New growth of fine-grained micas is not observed, however, suggesting that this cleavage developed at sub–greenschist facies conditions. This disjunctive cleavage is apparently cut or overprinted by 0.25–2-m-thick shear zones with non-coaxial fabrics that are locally developed along steeply NE-dipping mudstone-rich layers of the Big Creek conglomerate and are subparallel to the regional

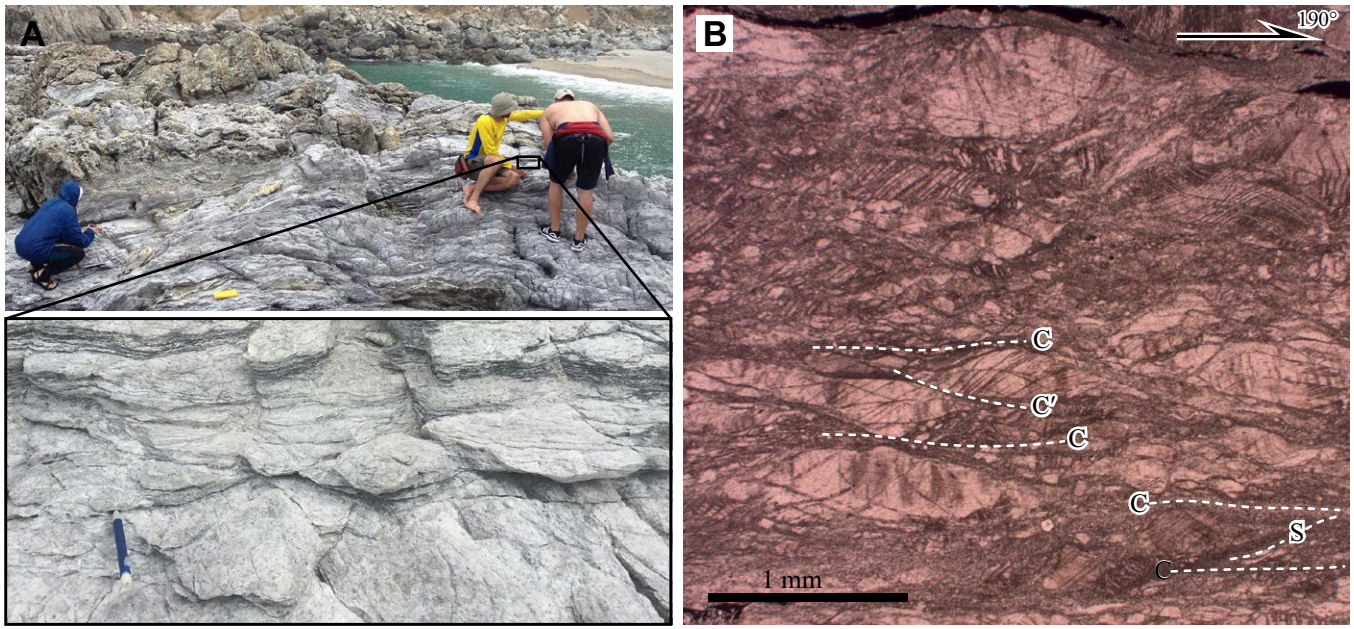

Figure 4. Photographs illustrating structural relationships along the McWay fault. (A) Mylonitic marbles exposed along the McWay fault at McWay Falls. Note mineral stretching lineation (parallel to long dimension of pencil) in enlarged view. (B) Plane-light photomicrograph illustrating marble microstructures including grain-size reduction along slip planes and non-coaxial (top-to-the-south) C′ shear bands and S-C fabrics.

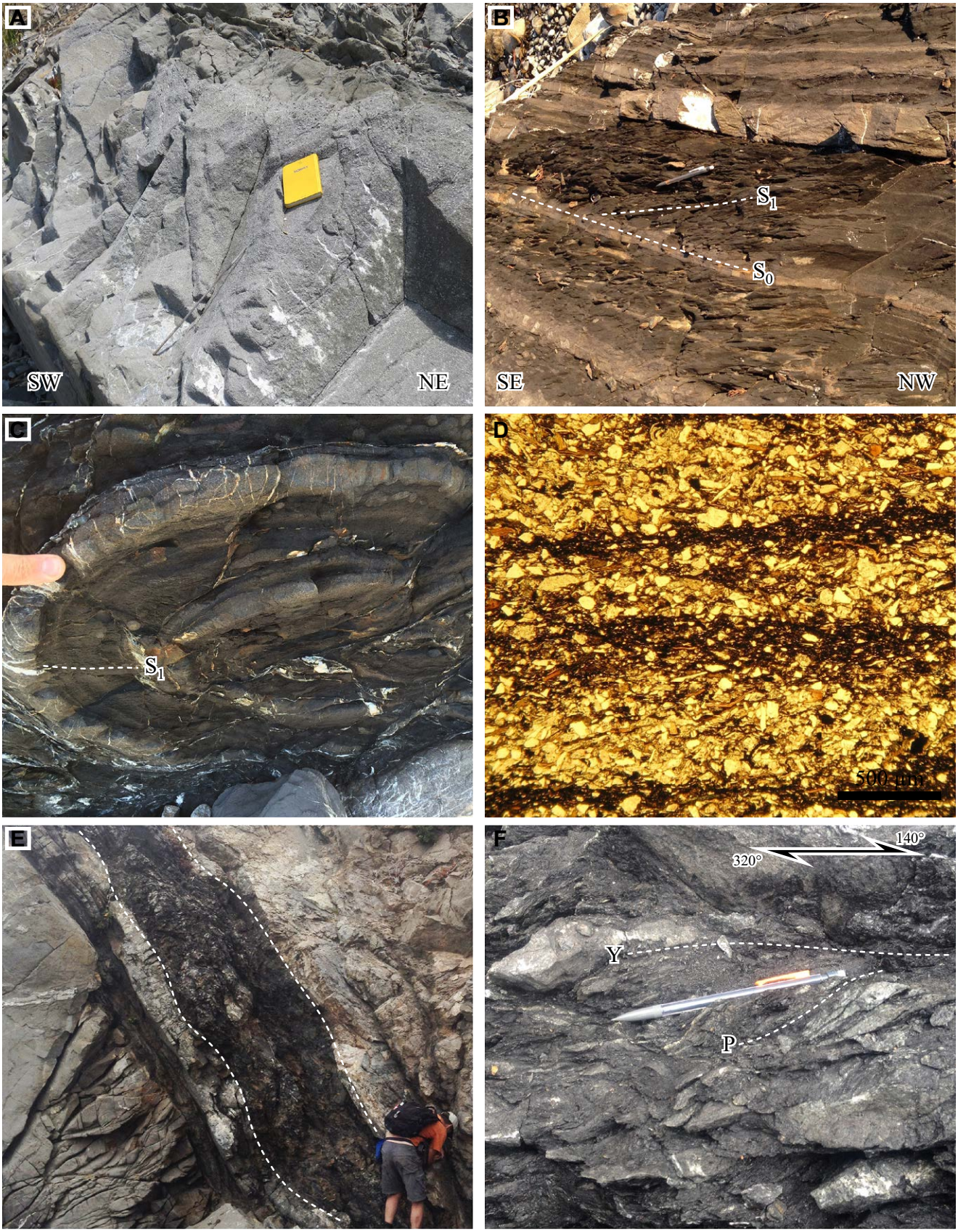

Figure 5. Photographs illustrating structural relationships in Salinian block Big Creek conglomerate. (A) Channel fill and graded sandstone beds fining up to the southwest demonstrating the overturned nature of the Big Creek conglomerate at Esalen Beach. Notebook dimensions are 165 cm × 11.5 cm. (B) Disjunctive cleavage developed in Big Creek conglomerate thinly laminated muds north of Esalen beach. S_0—bedding; S_1—cleavage. (C) Folded interlayers of Big Creek conglomerate mudstone and sandstone with axial planar cleavage. (D) Plane-light photomicrograph illustrating spaced disjunctive cleavage developed in the Big Creek conglomerate. (E) Shear zone (~1 m wide; dashed boundaries) with non-coaxial fabrics developed in Big Creek conglomerate mudstones. (F) Non-coaxial P-Y fabrics indicating dextral displacement in a shear zone cutting the Big Creek conglomerates.

strike of the Sur-Nacimiento fault (Figs. 3A, 5E). We use P-Y-R Riedel composite structure terminology (analogous to S-C-C′ fabrics in rocks that experienced crystal-plastic deformation, e.g., Cowan and Brandon [1994]) to describe the suite of planar fabrics developed in these non-coaxial shear zones. Slip vectors within these shear zones were estimated by determining the line within the Y-plane perpendicular to P-Y–plane intersection (e.g., Moore, 1978), and yield dominantly subhorizontal transport directions that are subparallel to brittlely developed slickenlines locally found on Y-planes (Fig. 3A). Non-coaxial fabrics in these shear zones including P-Y fabrics and asymmetric blocks consistently indicate subhorizontal dextral slip (Figs. 3A, 5F).

Outcrop-Scale Structure of the Franciscan Complex

Coastal exposures of Nacimiento-affinity Franciscan Complex within and south of the Sur-Nacimiento fault zone are found in beach surfaces, beach cliffs, and sea stacks. These fresh outcrops reveal an abundance of exotic blocks down to the centimeter scale hosted within a mudstone matrix that displays complex internal structure. Although individual blocks were not mapped as part of this work, exotic blocks identified within the field area include greywacke, thinly laminated sandstone and shale interbeds, bedded chert, conglomerate, pillow basalt, serpentinite, greenstone, greenschist, and rare blueschist. In addition, a unique block identified in the sea cliffs south of Dolan Point is characterized by a chaotic mixture of granitic cobbles, angular sandstone clasts, and greenstone inclusions set in a scaly mudstone matrix. Resistant blocks are abundantly cut by variably oriented brittle faults and at least one mylonitic shear zone (immediately north of the Big Creek Cove Salinian enclave), although the relative timing of and original orientations of these structures are unclear given the probability of multiple generations of deformation and subsequent rotation within individual blocks.

The matrix of the Franciscan Complex consists of dark scaly mudstone that displays an anastomosing shear fabric with NW-SE strike and moderately NE-dipping foliation throughout the field area (Figs. 3B, 6A, 6B). Shear zones with non-coaxial fabrics are developed within the mudstone matrix adjacent to large blocks and in more penetrative shear zones as much as 3 m wide. These more penetrative shear zones are subparallel to the regional trend of the matrix foliation in the Franciscan Complex, and are increasingly abundant adjacent to strands of the Sur-Nacimiento fault. Dominantly subhorizontal slip vectors in these penetrative shear zones are defined by mechanically aligned detrital micas within the muds, fibers associated with secondary vein mineralogy, and the P-Y–plane intersection. Non-coaxial fabrics within these penetrative shear zones <1 km from the main trace of the Sur-Nacimiento fault include P-Y fabrics and asymmetric blocks that consistently display dextral transport (Figs. 3B, 6C, 6D) and that are similar to shear zones with non-coaxial fabrics developed in Big Creek conglomerate mudstone. At distances >1 km from the main plane of the Sur-Nacimiento fault at Big Creek Cove, non-coaxial fabrics in penetrative shear zones are more variable. A 50-cm-thick shear zone that cuts a map-scale greenstone block yields thrust-sense slip, whereas a 3-m-thick shear zone observed along the margin of the Big Creek Cove Salinian enclave yields a dextral P-Y fabric that is overprinted by normal-sense slickenlines associated with clay gouge development (Fig. 3B).

Structural Repetition of the Sur-Nacimiento Fault Zone

In the vicinity of Big Creek, the Salinian block–Nacimiento block contact is repeated at least five times, yielding a complicated map pattern with isolated slivers, or enclaves, of rocks of Salinian affinity fully enclosed within Nacimiento Franciscan Complex, and Nacimiento Franciscan Complex enclosed within rocks of Salinian affinity. The main plane of the Sur-Nacimiento fault intersects the coastline ~1 km south of Esalen; to its northeast, rocks of Salinian affinity include the Slate Rock Franciscan enclave, and to its southeast, rocks of Nacimiento affinity include fault-bounded slivers of Salinian rocks at Dolan Cove, Rat Creek, Dolan Point, Gamboa Ridge, and Big Creek Cove (Fig. 2; Plate S1 [footnote 1]). The main plane juxtaposes overturned Big Creek conglomerate against sheared Franciscan mud matrix mélange, and is delineated by a roughly NW-SE–striking zone of clay gouges ~4 m thick that crops out beneath boulders on the beach surface and below Quaternary landslides and terrace deposits in the beach cliff. This gouge is composed primarily of crushed Franciscan Complex mudstone, although it also includes cobble-sized clasts of tonalite and greenstone of Salinian and Nacimiento affinity, respectively. The location of this gouge is aligned with the regional NW-SE trend of the main plane of the Sur-Nacimiento fault in the hillslopes above State Route 1 at Dolan Creek and with a prominent band of tectonized serpentinite of Nacimiento affinity that separates the Dolan Point Salinan enclave from the Salinian block basement mapped in the Big Creek drainage (Norris, 1985; Hall, 1991; Dibblee and Minch, 2007a). Immediately to the south of the gouge along the main plane of the Sur-Nacimiento fault, Franciscan mud matrix mélange displays dextral asymmetric fabrics developed within a moderately NE-dipping scaly foliation (see description of Franciscan structure below).

North of the main plane of the Sur-Nacimiento fault, the Slate Rock Franciscan enclave is composed of intensely sheared Franciscan Complex mud matrix ~20 m thick perpendicular to its foliation and which is sandwiched between exposures of Big Creek conglomerate strata. The Franciscan mud matrix within this enclave includes abundant lenses of greenschist that range from centimeter-scale stringers within the foliation to larger bodies as much as 0.5 m thick and 3 m along the foliation. Similar to the gouge zones along the main plane of the fault, the mud matrix mélange within the Slate Rock Franciscan enclave also includes rounded tonalite clasts as large as 5 cm in diameter. The northern contact of this enclave is characterized by moderately NNE-dipping mélange that is sharply juxtaposed against cobble conglomerate of the Big Creek conglomerate. The southern contact of the enclave grades gradually from sheared Franciscan mud matrix into semi-ductile gouge zones within interlayered sands and muds of the Big Creek conglomerate that become progressively less deformed within the package of rocks that stretches 50 m to the south of the enclave. Foliation within the enclave and in semi-ductile

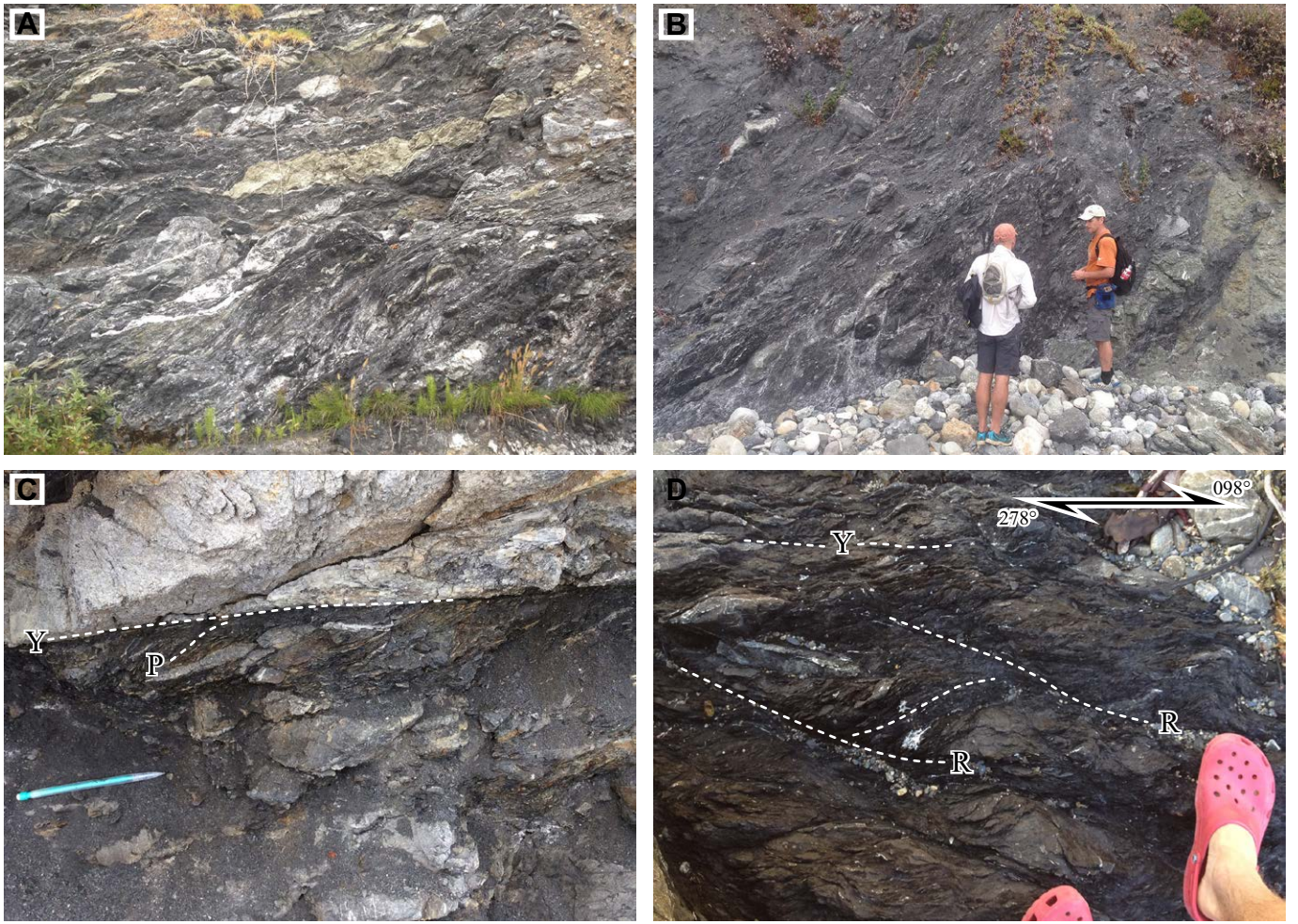

Figure 6. Photographs illustrating structural relationships in Nacimiento block Franciscan Complex. (A) Foliated Franciscan mud matrix mélange with bodies of lenticular greenschist at Dolan Cove; greenschist body is ~1.5 m in length. (B) Shear zone with non-coaxial structures developed parallel to regional foliation within Franciscan Complex mélange. (C) Non-coaxial P-Y fabrics indicating dextral slip in a shear zone developed adjacent to a block of sandstone in Franciscan Complex mélange near Dolan Cove. (D) Slip planes (Y) and shear bands inclined in the direction of slip (R) indicating non-coaxial dextral slip in a shear zone developed within the Slate Rock Franciscan enclave.

gouge zones of the Big Creek conglomerate display subhorizontal lineations and abundant P-Y fabrics indicating dextral shear sense. However, the foliation within the Slate Rock Franciscan enclave dips moderately N and obliquely to the trend of the main plane of the Sur-Nacimiento fault.

South of the main plane of the Sur-Nacimiento fault, the Dolan Cove Salinian enclave crops out on the two headlands immediately north of Dolan Creek and is fully enclosed within Nacimiento mélange. These Salinian rocks are defined by NW-SE–striking, subvertical beds of Big Creek conglomerate with rare siltstone and sandstone interlayers, and at Dolan Creek, this enclave is only 10–20 m wide. The contacts of this enclave are poorly exposed, although black gouge was identified beneath boulders on the beach along its northeast contact at Dolan Creek, and Franciscan mud matrix on either side of the enclave is

pervasively sheared along NE-dipping foliation planes that commonly display dextral shear-sense fabrics. Based on the map pattern, the contacts of the Dolan Cove Salinian enclave are parallel to the main plane of the Sur-Nacimiento fault, with a NW-SE trend and subvertical dip. Farther to the southwest along this trend and higher on the Big Sur hillslopes, the Dolan Cove Salinian enclave is aligned with poorly exposed Salinian-affinity outcrops that define the Rat Creek and Dolan Point Salinian enclaves (Fig. 2; Plate S1 [footnote 1]).

The Gamboa Ridge Salinian enclave (Norris, 1985; the Big Creek Salinian enclave of Dickinson et al., 2005) is the largest Salinian enclave in the region and consists of a variety of Salinian basement rocks and overlying Big Creek conglomerate within the University of California Big Creek Reserve. This Gamboa Ridge Salinian enclave crops out on the hillslopes above the Big Sur coast and was not investigated in detail as part of this study. However, map patterns from previous work suggest a moderately NE-dipping fault along its southwestern contact and a NW-SE–striking fault with a subvertical dip along its northeastern contact (Seiders et al., 1983; Norris, 1985; Hall, 1991; Dibblee and Minch, 2007a). Norris (1985) mapped this steeply dipping northeastern contact as a fault that intersects the beach cliffs just to the north of Dolan Rock, although the rocky coastline at this location precluded direct observation of the structure during this study.

The Big Creek Cove Salinian enclave of Norris (1985) crops out along the beach cliffs just to the south of the bridge that crosses Big Creek, and consists of pervasively sheared Salinan basement tonalites that crop out between blocks of Franciscan pillow basalts and metavolcanic rocks. The northern contact of the Big Creek Cove Salinian enclave is not exposed, although the southern contact is marked by an ~4-m-wide zone of fault gouge. The gouge zone displays a sharp contact between structurally higher, tan clay gouge adjacent to Salinian basement and black clay gouge structurally lower and adjacent to Franciscan assemblages of the Nacimiento block. When excavated, the contact between tan and black gouges reveals a delicate slip surface in clay gouge that strikes 330° with a dip of 72°NE and roughly down-dip lineations. Foliation patterns in the gouge suggest that the most recent displacement within the gouge was northeastern-side-down, normal-sense slip (Fig. 3B, overprint on contact). However, resistant blocks within the black gouge with steeply N-dipping orientations may represent P planes indicating a previous generation of subhorizontal dextral slip within the gouge zone (Fig. 3B, blocks in gouge). Farther to the south of the Big Creek Cove Salinian enclave, multiple zones of discontinuous black gouge were identified beneath terrace deposits and landslides in the cliff faces above the beach, although poor exposure precluded further investigation of these gouges.

KINEMATIC ANALYSIS OF OUTCROP-SCALE SHEAR ZONES AND FAULTS

Kinematic analysis of outcrop-scale structures can be used to get a better understanding of regional strain patterns. In this section, we present P- and T-axes (shortening and extension axes) determined from shear zones with non-coaxial structures and brittle faults developed within or adjacent to the Sur-Nacimiento fault zone from McWay Falls to Mill Creek. P- and T-axes were calculated using Richard Allmendinger's FaultKin 6 software (http://www.geo.cornell.edu/geology/faculty/RWA/programs/faultkin.html) based on the science and algorithms of Allmendinger et al. (2012) and Marrett and Allmendinger (1990).

Kinematic analysis of 26 different shear zones with non-coaxial structures observed <1 km from the strike of the main plane of the Sur-Nacimiento fault yields generally subhorizontal E-W–trending T-axes and subhorizontal N-S–trending P-axes consistent with dextral displacement along the NW-SE–striking Sur-Nacimiento fault (Plate S1 [footnote 1]; Fig. 7A). When differentiated by their host rock type, steeply NE-dipping shear zones with subhorizontal lineations developed in the Big Creek conglomerate yield shallowly S-plunging P-axes and E-W–trending T-axes with shallow to moderate plunges. In contrast, shear zones developed in the Franciscan Complex matrix display more moderate dips that trend more toward the NNE, and yield P-axes with shallow to moderate plunges to the S and SE and T-axes that cluster with moderate plunges toward the WSW. Farther south, and >1 km from the trend of the main plane of the Sur-Nacimiento fault, shear zones observed in the Franciscan Complex at Big Creek Cove are more variable (Plate S1 [footnote 1]; Fig. 7A). Shallowly NNE-dipping shear zones that cut a map-scale greenstone block yield moderately E-plunging T-axes and moderately WSW-plunging P-axes consistent with ENE-WSW shortening. In contrast, normal-sense displacement within the clay gouge zone developed along the western boundary of the Big Creek Cove Salinian enclave yields subvertical P-axes and shallowly NE-plunging T-axes consistent with SW-NE extension (Plate S1 [footnote 1]).

Discrete brittle fault surfaces are ubiquitously developed in coastal and hillside exposures from McWay Falls to Mill Creek. These brittle structures are found in all rock types at a range of scales displaying centimeters to tens of meters of displacement, and with diverse orientations that variably cut as well as reactivate preexisting bedding, foliation, and ductile shear surfaces (Fig. 7B). The morphology of these faults is also diverse, with fault surfaces that are alternately characterized by polished surfaces with grooved slickenlines or by surfaces with abundant slickenfibers formed by mineralization along the fault. Fault surfaces with strikes within 20° of the average strike of the Sur-Nacimiento fault (134° [SE] or 314° [NW]) from Esalen to Mill Creek are dominantly subvertical with subhorizontal slickenlineations (Fig. 7B). Structures observed to determine fault slip sense include offset marker beds, slickenfiber steps, and Riedel shears; out of 349 discrete fault surfaces measured within the field area, 207 displayed reliable slip-sense indicators (Fig. 7C). Despite the geometric and kinematic diversity of these faults, kinematic axes are similar across different outcrops, with dominantly subhorizontal, WNW-ESE–trending T-axes, and P-axes that define a weak NNE-SSW girdle with tighter concentrations that cluster with subhorizontal orientations. When sorted by orientation, the majority of steeply plunging P-axes are found on faults striking >20° from the average trend of the Sur-Nacimiento fault, whereas surfaces within 20° of the Sur-Nacimiento fault yield subhorizontal P- and T-axes (Fig. 7C). These re-

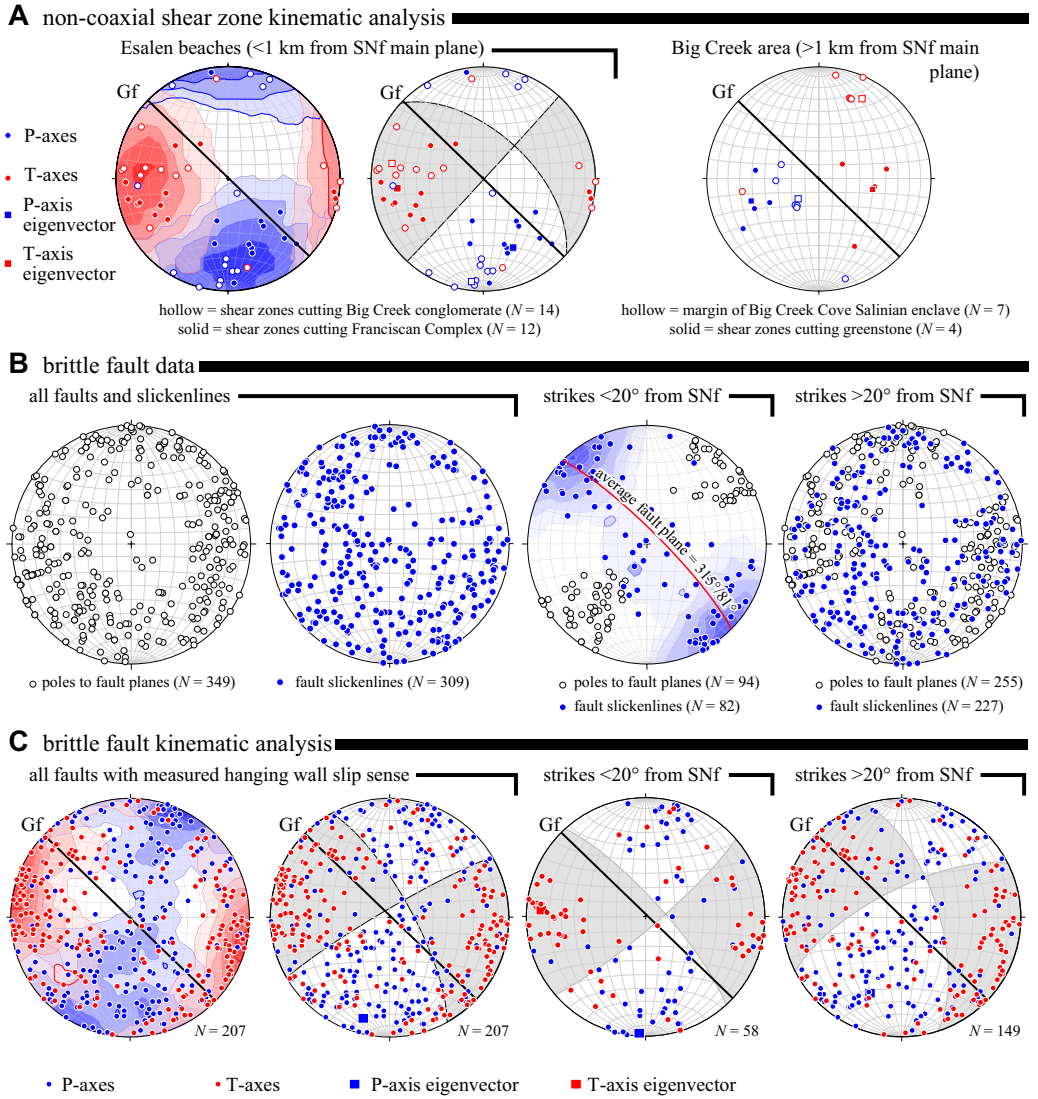

Figure 7. (A) Kinematic analysis of shear zones with non-coaxial fabrics. Shear zone orientations and lineations used to determine P- and T-axes are plotted in Figure 3. (B) Compilation of all brittle fault data from McWay Falls to Mill Creek. (C) Kinematic analysis of brittle faults displayed in B. All plots are lower-hemisphere, equal-area stereonet diagrams. Thick black plane on kinematic plots in A and C represents the average strike of the subvertical Gamboa fault system (314° [NW] or 134° [SE]) from Esalen beach to Mill Creek. Contours are Kamb; gray-shaded quadrants illustrate fault plane solutions from P- and T-axis maximum eigenvectors that were determined through linked Bingham analysis. Notation for average plane orientations refers to strike azimuth°/dip plunge°. Gf—Gamboa fault; SNf—Sur-Nacimiento fault.

sults are generally compatible with dextral slip along steeply dipping fault surfaces subparallel to the SE-NW–striking Sur-Nacimiento fault with a component of oblique dextral-normal slip that is accommodated along fault surfaces with orientations at higher angles to the Sur-Nacimiento fault. When sorted by location, subtle variations in P- and T-axis orientations are observed, but the general pattern of dextral slip along NW-SE–striking faults dominant (Plate S1 [footnote 1]). One notable exception to this pattern is the set of NW-striking sinistral faults observed in upper Big Creek conglomerate along Highway 1 at Esalen that yield subhorizontal T- and P-axes with NNE-SSW and ESE-WNW trends. These faults contrast sharply with the set of NNW-SSE–striking faults above Highway 1 at Dolan Creek just 2 km to the south that indicate oblique dextral-normal slip.

DISCUSSION

Salinian Enclaves and Dextral Reactivation of the Sur-Nacimiento Fault

A primary finding of this study is evidence for dextral displacement adjacent to the Salinian-Nacimiento terrane boundary that is documented by shear zones with non-coaxial fabrics and brittle fault surfaces indicating dominantly WNW-ESE extension and NNE-SSW shortening. This strain pattern supports the hypothesis that the Salinian enclaves near Big Creek developed during dextral slip along a subvertical, NW-SE–striking fault zone or suite of faults that cut and/or reactivated portions of the older Sur-Nacimiento fault responsible for the original juxtaposition of the Salinian and Nacimiento blocks (Fig. 2D; e.g., Dickinson et al., 2005). This interpretation is consistent with previous regional-scale mapping efforts that link the 6.5-km-long Gamboa Ridge Salinian enclave via the Gamboa fault to Salinian rocks that are abutted against a linear segment of the Sur-Nacimiento fault that stretches 6.25 km from Limekiln Creek to Mill Creek (Fig. 2; Seiders et al., 1983; Dibblee and Minch, 2007a, 2007b). The lack of mapped Big Creek conglomerate above Salinian basement near Limekiln Creek presents a problem for this reconstruction, although this apparent mismatch may be explained by the limited aerial extent of the Big Creek conglomerate and/or the poor outcrop potential of the Big Creek conglomerate on the densely vegetated Big Sur hillslopes that make its recognition difficult without detailed mapping. Using this correlation as a piercing point suggests dextral displacement of 8–9 km along the Gamboa fault, and offset of the Dolan Point Salinian enclave from exposures of Big Creek conglomerate east of the main plane of the Sur-Nacimiento fault farther south allows for an additional 1–2 km of dextral displacement (e.g., Dickinson et al., 2005, their figure 8); together, these correlations suggest 8–11 km of total dextral displacement within this broader Gamboa fault zone.

The younger age limit for slip on the Sur-Nacimiento fault is typically cited as early Miocene based on Oligocene–lower Miocene Vaqueros Formation that overlies the fault west of Atascadero (Graham, 1978; Dickinson et al., 2005) (Fig. 1). Similarly, while compilations of Quaternary fault activity suggest some Quaternary displacement in the vicinity of Big Creek, sections of the Sur-Nacimiento fault southeast of Mill Creek are considered inactive (Jennings and Bryant, 2010). However, compilations of recent central California coast seismic activity yield numerous events along the Sur-Nacimiento fault in the vicinity of Big Creek (Clark and Rosenberg, 1999; McLaren and Savage, 2001; Hardebeck, 2010) (Fig. 8A). Available fault-plane solutions determined from these events yield dominantly dextral strike-slip mechanisms (McLaren and Savage, 2001; Hardebeck, 2010) that are similar to the average fault-plane solution determined from non-coaxial shear zones with gouge (Fig. 8B). In contrast, the NNE-SSW P-axis girdle associated with late brittle faults near Big Creek is suggestive of dextral strain with a component of normal slip, which is inconsistent with the regional nature of transpressional strain that is expected adjacent to the San Simeon segment of the San Gregorio–San Simeon–Hosgri fault (e.g., Johnson et al., 2018). However, minor faults with normal displacement have been noted before along the Big Sur coast (Trasko and Cloos, 2007), and this subtle component of normal strain may (1) indicate that dextral displacement along the Gamboa fault initiated as early as the Miocene when the predominant strain pattern throughout the central California coast was transtensional (e.g., Graham, 1978; Colgan et al., 2012), or (2) be related to localized transtensional strain associated with releasing bends developed along the Gamboa fault (e.g., at Dolan Creek: Plate S1 [footnote 1]; south of Partington Point: Johnson et al., 2018, their figure 11). Regardless, given the similar dominantly dextral pattern of strain associated with recent seismic events and with non-coaxial shear zones and brittle faults along the Gamboa fault, we suggest that the 8–11 km of dextral slip along the Gamboa fault is Miocene and younger, and that the fault may be currently active. This hypothesis suggests that preexisting weaknesses along the Salinian-Nacimiento terrane boundary—possibly related to rheology contrasts across the boundary or to strain-weakened rocks within the Sur-Nacimiento fault—may have localized a regionally significant component of post-Oligocene dextral displacement.

South of San Simeon, historic seismicity and aftershocks of the A.D. 2003 San Simeon earthquake (M_w 6.5) yield dextral-reverse and reverse focal mechanisms along the Sur-Nacimiento fault near its southern intersection with the Oceanic–West Huasna fault, and indicate north-directed backthrusting beneath the fault trace of the Sur-Nacimiento fault (McLaren and Savage, 2001; McLaren et al., 2008; Fig. 8B). We suggest that this variability in strain observed in reactivated segments of the Sur-Nacimiento fault north of San Simeon at Big Creek (e.g., dominantly dextral strain along the Gamboa fault) and south of San Simeon could be the result of one of, or a combination of, two end-member models (Fig. 8).

(1) The Gamboa fault may be one of a system of fault splays at the southern tip of the San Gregorio fault that transmit the majority of dextral strain from the San Gregorio fault to the San Simeon fault in the more continuous San Gregorio–San Simeon–Hosgri fault system (e.g., Clark and Rosenberg, 1999). This model predicts that slip along the Gamboa fault should decrease abruptly to the south, and that backthrusts that surface within the Sur-Nacimiento fault south of San Simeon are related to pop-up structures associated with thrust displacement along the Oceanic fault (e.g., McLaren et al., 2008) that are localized by preexisting weaknesses along the Salinian-Nacimiento terrane boundary (Fig. 8A). This model is supported by the absence of mapped Quaternary faults (Jennings and Bryant, 2010) and apparent lack of microseismicity between Mill Creek and San Simeon on the Sur-Nacimiento fault (McLaren and Savage, 2001; Hardebeck, 2010).

(2) Alternatively, the Gamboa fault may be one of several faults that reactivate the Sur-Nacimiento fault zone and transmit a minor component of San Gregorio fault dextral strain southward along the Salinian-Nacimiento terrane boundary. This model predicts that reactivated segments of the Sur-Nacimiento fault are primarily dextral north of

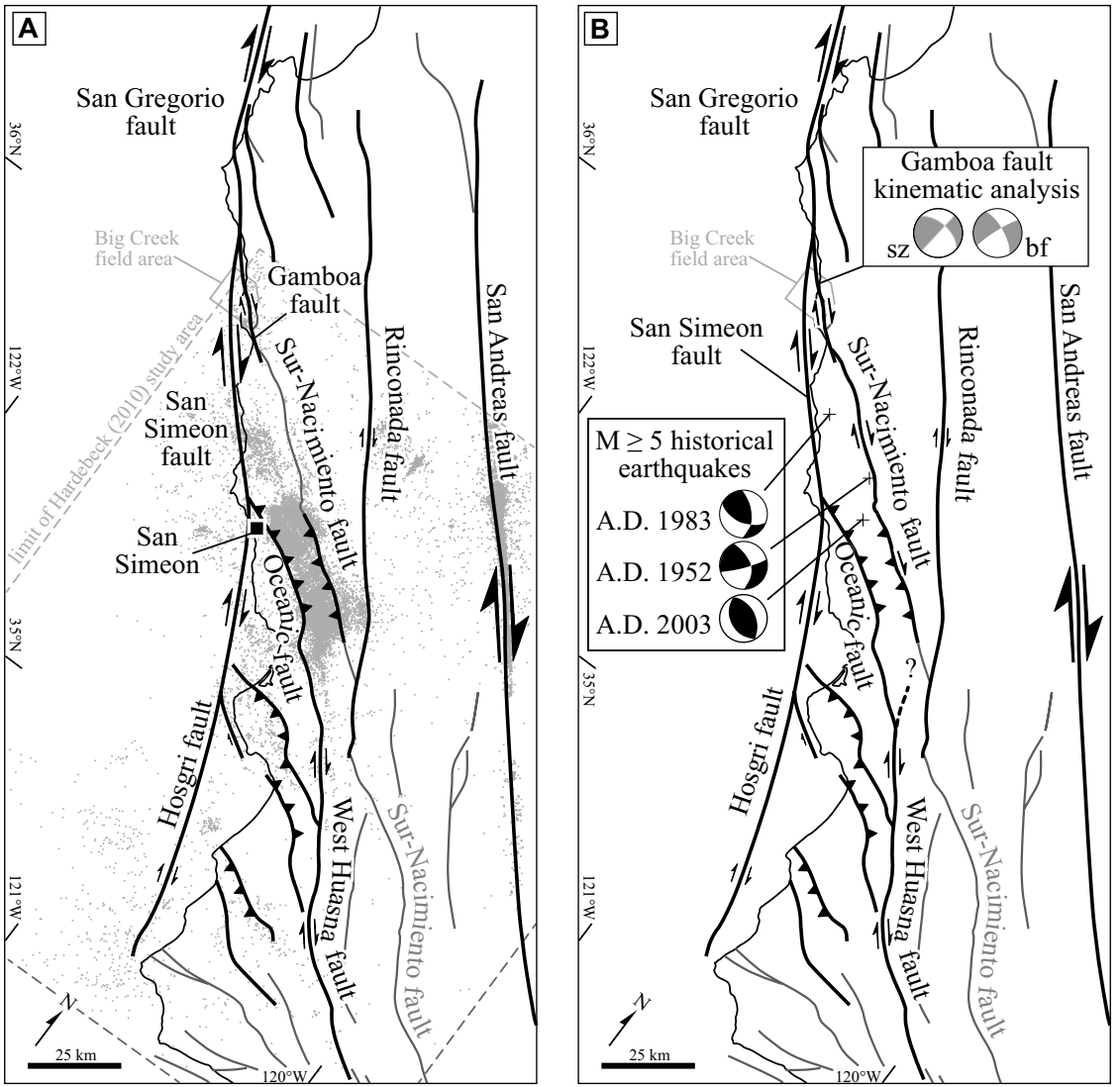

Figure 8. Fault maps illustrating the regional significance of models for the southern continuation of Miocene and younger dextral slip on the Gamboa fault. Faults and slip senses are after Hardebeck (2010): active faults with significant slip are drawn with thick black lines; faults with less-significant slip are drawn in gray; size of transform arrows is meant to schematically represent cumulative slip. (A) Gamboa fault slip is transferred to the San Simeon fault. Gray dots indicate instrumentally recorded California Integrated Seismic Network catalog earthquake locations from 1987 to 2008 (from Hardebeck, 2010). (B) Gamboa fault slip is transferred to older structures developed along the Sur-Nacimiento fault. Focal mechanisms and locations for historical earthquakes M ≥ 5 are from McLaren and Savage (2001); fault plane solutions from the Gamboa fault are from shear zones (sz) and brittle faults (bf) illustrated in Figure 7 (this study).

San Simeon, and the southward increase in dextral-reverse slip may be explained by pop-up structures related to the convergence of the Sur-Nacimiento fault zone with the reverse-dextral Oceanic fault (Fig. 8B). This model is supported by the nearly purely dextral A.D. 1952 Bryson earthquake (M_L 6.2) recorded along the Sur-Nacimiento fault zone just north of San Simeon (McLaren and Savage, 2001).

Estimates for slip on the San Gregorio–San Simeon–Hosgri fault system indicate a progressive reduction in dextral slip between the San Gregorio fault north of Big Creek and the San Simeon and Hosgri faults south of Big Creek (see Langenheim et al., 2013, and references therein). This southward slip reduction suggests that northward translation of rocks west of the San Gregorio–San Simeon–Hosgri fault is gradually transferred to structures dis-

tributed throughout the Nacimiento block, although the locations and mechanisms of these structures within the Nacimiento block are debated (McLaren and Savage, 2001; Lettis et al., 2004; Dickinson et al., 2005; Colgan and Stanley, 2016). Most published models for Nacimiento block strain are consistent with model 1, presented above (Fig. 8A), in which there is no significant post-Oligocene reactivation of the Sur-Nacimiento fault zone, and Nacimiento block strain is distributed throughout several discrete domains south of the Oceanic fault (McLaren and Savage, 2001; Lettis et al., 2004) or is limited to the Santa Maria Basin (Dickinson et al., 2005). These models emphasize the significance of dextral slip on the West Huasna fault and dextral-reverse slip on the Oceanic fault to accommodate space problems north of San Simeon in reconstructions of the northern Nacimiento block (e.g., Langenheim et al., 2013). Alternatively, Hardebeck (2010) cited evidence for recent thrust reactivation of the Sur-Nacimiento fault indicating Nacimiento block strain north of the Oceanic fault. This assertion is more consistent with model 2, presented above (Fig. 8B), and with the interpretation that 15–30 km of dextral slip on the West Huasna fault (Hall and Saleeby, 2013; Langenheim et al., 2013) may be partitioned northward into predominantly reverse and dextral components of slip on the Oceanic fault and reactivated segments of the Sur-Nacimiento fault, respectively. Ultimately, further resolution of the two end-member models presented here for the southward transfer of San Gregorio fault dextral slip has significant implications for the seismic hazards of the central California coast.

Pre-Miocene Structure of the Sur-Nacimiento Fault Zone and Adjacent Rocks

Despite the evidence for recent reactivation of the Sur-Nacimiento fault zone, the rocks from McWay Falls to Gamboa Point preserve geometric relationships and fabrics that provide insight into the pre-Miocene structure of the Sur-Nacimiento fault and the original mechanism for Salinian-Nacimiento block juxtaposition. At the map scale, previous work has focused on the original orientation of the Sur-Nacimiento fault: assertions that the Salinian enclaves at Big Creek are klippe that preserve Salinian rocks in the hanging wall of a low-angle fault (Hall, 1991) support either thrust (Hall, 1991; Hall and Saleeby, 2013) or normal (Chapman et al., 2016) displacement (Fig. 2B), whereas linear segments of the Salinian-Nacimiento contact support a subvertical fault with either sinistral or dextral strike-slip displacement (Figs. 2C, 2D; e.g., Dickinson et al., 2005). Our interpretation that the Salinian enclaves in the vicinity of Big Creek were formed as the result of recent dextral displacement within steeply dipping strands of the Gamboa fault zone disputes the assertion by Hall (1991) that the Gamboa Ridge and Dolan Point Salinian enclaves are fault klippe. However, the Salinian-Nacimiento terrane boundary along the western margin of the Gamboa Ridge Salinian enclave dips 30°–50°NE (e.g., Seiders et al., 1983; Hall, 1991); with this Salinian enclave restored to its original position adjacent to Limekiln Creek, the circuitous map pattern of the terrane boundary from Big Creek to Mill Creek is most consistent with a moderately NE-dipping Sur-Nacimiento fault prior to recent dextral reactivation (Fig. 2D). This map pattern contrasts sharply with the linear segment of the Sur-Nacimiento fault south of Mill Creek (Fig. 1) and with geophysical evidence suggesting a steeply NE-dipping terrane boundary north of San Simeon (Langenheim et al., 2013; Graymer et al., 2014). Further work is needed along the Salinian-Nacimiento terrane boundary to determine if other subvertical segments of the boundary may reflect recent dextral reactivation of the Sur-Nacimiento fault rather than the fault's original geometry, or if the low-angle Big Creek segment of the Sur-Nacimiento fault is a regional outlier.

At the outcrop scale, our field observations indicate that recent brittle gouge zones cut and locally reactivate earlier structures along the Sur-Nacimiento fault. Dextral shear zones in Franciscan mud matrix mélange dip moderately toward the NNE and parallel regional foliation. Moderately NE-dipping foliation planes in the mélange may support the interpretation that Salinian-Nacimiento block juxtaposition occurred along an originally low angle Sur-Nacimiento fault. However, moderately NE-dipping foliation planes are observed elsewhere in the Nacimiento block within the Santa Lucia Range (e.g., Singleton and Cloos, 2013), and the timing of this regionally developed foliation is poorly constrained. Given these poor timing constraints, this moderately NE-dipping foliation could potentially be related to a variety of deformation events: (1) Late Cretaceous tectonism within the growing accretionary complex, (2) younger Late Cretaceous–Paleocene reactivation of the mélange associated with a low-angle Sur-Nacimiento fault (Chapman et al., 2016; Hall, 1991; Hall and Saleeby, 2013), (3) Eocene–Oligocene dextral wrenching (e.g., discussion below; Vedder et al., 1991), or even (4) Quaternary reverse-dextral shearing associated with uplift of the Santa Lucia Range in the hanging wall of the Oceanic fault (Hardebeck, 2010). Sinistral slip is conspicuously absent from this list of possibilities, although given the rheologically weak nature of the mud-matrix mélange, transposition of a preexisting sinistral fabric cannot be ruled out. As such, we do not consider the fabrics in the Franciscan mélange to be diagnostic of a single deformation event along this stretch of the Sur-Nacimiento fault.

In the Salinian block, shear zones with non-coaxial fabrics preferentially reactivate overturned beds and cut the WNW-ESE–striking disjunctive cleavage that characterizes the Big Creek conglomerate in the footwall of the top-to-the-south McWay fault. These structures are similar in orientation to previously mapped WNW-ENE–trending folds in the Big Creek conglomerate in the hanging wall of the McWay fault (Hall, 1991; Dibblee and Minch, 2007a), and are cumulatively consistent with N-S to NE-SW shortening or progressive dextral transpression adjacent to the Sur-Nacimiento fault. Type II and IV calcite twins and recrystallized calcite with mean grain sizes of 6–7 μm observed in marble mylonites on the McWay fault are typical of calcite deformation at temperatures of 250–300 °C (Ferrill et al., 2004; Ebert et al., 2008). These marble mylonites are thermally comparable to the disjunctive cleavage developed in Big Creek conglomerate mudstone, which lacks synkinematic mica growth, and are consistent with deformation at sub–greenschist facies temperatures of 200–300 °C. These temperatures of deformation are higher than elsewhere in the Santa Lucia Range where Salinian basement and overlying Late Cretaceous–Neogene strata have been at temperatures below which fission tracks

anneal in apatite (~100 °C) since the Late Cretaceous (Naeser and Ross, 1976; Colgan et al., 2012). Low-temperature thermochronology clearly indicates that this event must have occurred prior to 6 Ma when Salinian basement adjacent to the Gamboa fault at Limekiln Creek was at ~110 °C (Ducea et al., 2003). However, because the northern Salinian block was characterized by a transtensional tectonic setting recorded by early Miocene basins that cover much of the northern Salinian block (Graham, 1978; Colgan et al., 2012), we suggest that these sub–greenschist facies contractional structures are pre-Miocene. As an alternative to achieving sub–greenschist facies temperatures through contraction and tectonic burial alone, it is possible that these elevated temperatures could be related to a local thermal perturbation associated with the Los Burros mining district. Still, a latest Eocene(?) age for this auriferous hydrothermal event (Underwood et al., 1995) again suggests that this contractional event adjacent to the Sur-Nacimiento fault was pre-Miocene. The older age limit of sub–greenschist facies contractional fabrics is constrained by the Maastrichtian depositional age of the Big Creek conglomerate.

Given these Maastrichtian–Oligocene age constraints for sub–greenschist facies contraction within the Salinian block, it is possible that this event was associated with dextral transpression during the original juxtaposition of the Salinian and Nacimiento blocks along the Sur-Nacimiento fault. However, detrital zircon provenance studies of Nacimiento block trench and forearc basin sediments suggest an origin in southern California, and argue against allochthonous dextral transport of the Nacimiento block accretionary complex and forearc basin within the southern California late Mesozoic margin (Chapman et al., 2016; Johnston et al., 2018). As such, we suggest that this contractional event may have been associated with an enigmatic phase of Paleogene dextral displacement along the central California margin (Vedder et al., 1991; Sharman et al., 2013) possibly related to an increased component of dextral transport during the final stages of Farallon subduction (Doubrovine and Tarduno, 2008).

CONCLUSIONS

We mapped beach exposures and collected fault kinematic data from the Big Sur coast from McWay Falls to Gamboa point to place new constraints on the evolution of the Sur-Nacimiento fault. Key findings of this work include: (1) a sub–greenschist facies N-S to NE-SW contractional event preserved in the Salinian block adjacent to the fault associated with top-to-the-south thrust displacement on the McWay fault, a WNW-ESE–striking disjunctive cleavage, and overturned bedding in the Big Creek conglomerate; (2) a regionally developed NE-dipping foliation in Nacimiento block Franciscan mud matrix mélange; (3) repetitions of the Salinian-Nacimiento block terrane boundary that coincide with subvertical, NW-SE–striking shear zones; (4) NW-SE–striking shear zones with dextral non-coaxial structures that reactivate preexisting structures in the Salinian and Nacimiento blocks; and (5) brittle fault surfaces exposed throughout the field area that indicate dominantly WNW-ESE extension and NNE-SSW shortening.

Based on these data, we infer that Salinian enclaves within the Nacimiento block formed via Miocene and younger dextral displacement within the Gamboa fault zone that cut a moderately NE-dipping segment of the Sur-Nacimiento fault and transported Salinian-affinity rocks 8–11 km to the northwest. A better understanding of where dextral strain along the Gamboa fault is transferred toward the south—either to the San Simeon fault or to the Salinian-Nacimiento terrane boundary—is important for our understanding of the slip budget along the San Gregorio–San Simeon–Hosgri fault, and for seismic hazard assessment of the central California coast. Although this recent dextral displacement obscures the original mechanism for Salinian-Nacimiento block juxtaposition along the Sur-Nacimiento fault, pre-Miocene contractional structures and fabrics preserved in the Salinian block may be representative of a period of Paleogene dextral transpression adjacent to the Salinian-Nacimiento terrane boundary. This data set highlights the multiple episodes of deformation along the Salinian-Nacimiento terrane boundary and the Sur-Nacimiento fault, and underscores the importance of inherited structures with respect to our understanding of the modern tectonic setting of southern California.

ACKNOWLEDGMENTS

Funding for this project was supported by U.S. Geological Survey EdMap award number G15AC00177 granted to Johnston, and U.S. National Science Foundation grant EAR-1062720 awarded to Chapman. The authors thank the editorial staff at *Geosphere*, Darrel Cowan, and Robert McLaughlin for constructive manuscript reviews, in addition to the staff at the Esalen Institute for providing access to beaches near Hot Spring Creek, the staff at the University of California Big Creek Reserve for their excellent accommodations and access to their dive boat, and Devona Yates for piloting the dive boat during the course of our field work.

REFERENCES CITED

Allmendinger, R.W., Cardozo, N., and Fisher, D.M., 2012, Structural Geology Algorithms: Vectors and Tensors: Cambridge, UK, Cambridge University Press, 302 p.

Bennett, R.A., Wernicke, B.P., Niemi, N.A., Friedrich, A.M., and Davis, J.L., 2003, Contemporary strain rates in the northern Basin and Range province from GPS data: Tectonics, v. 22, 1008, https://doi.org/10.1029/2001TC001355.

Chapman, A.D., Ducea, M.N., Kidder, S., and Petrescu, L., 2014, Geochemical constraints on the petrogenesis of the Salinian arc, central California: Implications for the origin of intermediate magmas: Lithos, v. 200–201, p. 126–141, https://doi.org/10.1016/j.lithos.2014.04.011.

Chapman, A.D., Jacobson, C.E., Ernst, W.G., Grove, M., Dumitru, T., Hourigan, J., and Ducea, M.N., 2016, Assembling the world's type shallow subduction complex: Detrital zircon geochronologic constraints on the origin of the Nacimiento block, central California Coast Ranges: Geosphere, v. 12, p. 533–557, https://doi.org/10.1130/GES01257.1.

Clark, J.C., and Rosenberg, L.I., 1999, Southern San Gregorio fault displacement—Stepover segmentation vs. through-going tectonics: U.S. Geological Survey National Earthquake Hazards Reduction Program Final Technical Report, Grant Number 1434-HQ-98-GR-00007, 50 p.

Clark, J.C., Brabb, E.E., Greene, H.G., and Ross, D.C., 1984, Geology of Point Reyes Peninsula and implications for San Gregorio fault history, *in* Crouch, J.K., and Bachman, S.B., eds., Tectonics and Sedimentation along the California Margin: Pacific Section, Society for Sedimentary Geology (SEPM) Publication 38, p. 67–86.

Clift, P., and Vannucchi, P., 2004, Controls on tectonic accretion versus erosion in subduction zones: Implications for the origin and recycling of the continental crust: Reviews of Geophysics, v. 42, RG2001, https://doi.org/10.1029/2003RG000127.

Colgan, J.P., and Stanley, R.G., 2016, The Point Sal–Point Piedras Blancas correlation and the problem of slip on the San Gregorio–Hosgri fault, central California Coast Ranges: Geosphere, v. 12, p. 971–984, https://doi.org/10.1130/GES01289.1.

Colgan, J.P., McPhee, D.K., McDougall, K., and Hourigan, J.K., 2012, Superimposed extension and shortening in the southern Salinas Basin and La Panza Range, California: A guide to Neogene deformation in the Salinian block of the central California Coast Ranges: Lithosphere, v. 4, p. 411–429, https://doi.org/10.1130/L208.1.

Compton, R.R., 1960, Charnockitic rocks of the Santa Lucia Range, California: American Journal of Science, v. 258, p. 609–636, https://doi.org/10.2475/ajs.258.9.609.

Cowan, D.S., 1978, Origin of blueschist-bearing chaotic rocks in the Franciscan Complex, San Simeon, California: Geological Society of America Bulletin, v. 89, p. 1415–1423, https://doi.org/10.1130/0016-7606(1978)89<1415:OOBCRI>2.0.CO;2.

Cowan, D.S., and Brandon, M.T., 1994, A symmetry-based method for kinematic analysis of large-slip brittle fault zones: American Journal of Science, v. 294, p. 257–306, https://doi.org/10.2475/ajs.294.3.257.

Dibblee, T.W., and Minch, J.A., 2007a, Geologic map of the Lopez Point quadrangle, Monterey County, California: Dibblee Geological Foundation Map DF-363, scale 1:24,000.

Dibblee, T.W., and Minch, J.A., 2007b, Geologic map of the Partington Ridge quadrangle, Monterey County, California: Dibblee Geological Foundation Map DF-361, scale 1:24,000.

Dickinson, W.R., 1983, Cretaceous sinistral strike slip along Nacimiento Fault in coastal California: American Association of Petroleum Geologists Bulletin, v. 67, p. 624–645, https://doi.org/10.1306/03B5B66E-16D1-11D7-8645000102C1865D.

Dickinson, W.R., 2008, Accretionary Mesozoic–Cenozoic expansion of the Cordilleran continental margin in California and adjacent Oregon: Geosphere, v. 4, p. 329–353, https://doi.org/10.1130/GES00105.1.

Dickinson, W.R., Ducea, M., Rosenberg, L.I., Greene, H.G., Graham, S.A., Clark, J.C., Weber, G.E., Kidder, S., Ernst, W.G., and Brabb, E.E., 2005, Net Dextral Slip, Neogene San Gregorio–Hosgri Fault Zone, Coastal California: Geologic Evidence and Tectonic Implications: Geological Society of America Special Paper 391, 43 p., https://doi.org/10.1130/SPE391.

Doubrovine, P.V., and Tarduno, J.A., 2008, Revised kinematic model for the relative motion between Pacific oceanic plates and North America since the Late Cretaceous: Journal of Geophysical Research, v. 113, B12101, https://doi.org/10.1029/2008JB005585.

Ducea, M., House, M.A., and Kidder, S., 2003, Late Cenozoic denudation and uplift rates in the Santa Lucia Mountains, California: Geology, v. 31, p. 139–142, https://doi.org/10.1130/0091-7613(2003)031<0139:LCDAUR>2.0.CO;2.

Ebert, A., Harwegh, M., Berger, A., and Pfiffner, A., 2008, Grain coarsening maps for polymineralic carbonate mylonites: A calibration based on data from different Helvetic nappes (Switzerland): Tectonophysics, v. 457, p. 128–142, https://doi.org/10.1016/j.tecto.2008.05.007.

Ernst, W.G., 1970, Tectonic contact between the Franciscan mélange and the Great Valley sequence—Crustal expression of a late Mesozoic Benioff zone: Journal of Geophysical Research, v. 75, p. 886–901, https://doi.org/10.1029/JB075i005p00886.

Ernst, W.G., 1984, Californian blueschists, subduction, and the significance of tectonostratigraphic terranes: Geology, v. 12, p. 436–440, https://doi.org/10.1130/0091-7613(1984)12<436:CBSATS>2.0.CO;2.

Ernst, W.G., Snow, C.A., and Scherer, H.H., 2008, Contrasting early and late Mesozoic petrotectonic evolution of northern California: Geological Society of America Bulletin, v. 120, p. 179–194, https://doi.org/10.1130/B26173.1.

Ferrill, D.A., Morris, P.A., Evans, M.A., Burkhard, M., Groshong, R.H., Jr., and Onasch, C.M., 2004, Calcite twin morphology: A low-temperature deformation geothermometer: Journal of Structural Geology, v. 26, p. 1521–1529, https://doi.org/10.1016/j.jsg.2003.11.028.

Gilbert, W.G., 1971, Sur fault zone, Monterey County, California [Ph.D. thesis]: Stanford, California, Stanford University, 80 p.

Gilbert, W.G., and Dickinson, W.R., 1970, Stratigraphic variations in sandstone petrology, Great Valley sequence, central California coast: Geological Society of America Bulletin, v. 81, p. 949–954, https://doi.org/10.1130/0016-7606(1970)81[949:SVISPG]2.0.CO;2.

Graham, S.A., 1978, Role of Salinian block in evolution of San Andreas fault system: American Association of Petroleum Geologists Bulletin, v. 62, p. 2214–2231, https://doi.org/10.1306/C1EA53C3-16C9-11D7-8645000102C1865D.

Graymer, R.W., Langenheim, V.E., Roberts, M.A., and McDougall, K., 2014, Geologic and geophysical maps of the eastern three-fourths of the Cambria 30′ × 60′ quadrangle, central California Coast Ranges: U.S. Geological Survey Scientific Investigations Map 3287, scale 1:100,000, 47 p. text, https://doi.org/10.3133/sim3287.

Grove, K., 1993, Latest Cretaceous basin formation within the Salinian terrane of west-central California: Geological Society of America Bulletin, v. 105, p. 447–463, https://doi.org/10.1130/0016-7606(1993)105<0447:LCBFWT>2.3.CO;2.

Grove, M., Bebout, G.E., Jacobson, C.E., Barth, A.P., Kimbrough, D.L., King, R.L., Zou, H., Lovera, O.M., Mahoney, B.J., and Gehrels, G.E., 2008, The Catalina Schist: Evidence for middle Cretaceous subduction erosion of southwestern North America, *in* Draut, A.E., Clift, P.D., and Scholl, D.W., eds., Formation and Applications of the Sedimentary Record in Arc Collision Zones: Geological Society of America Special Paper 436, p. 335–362, https://doi.org/10.1130/2008.2436(15).

Hall, C.A., Jr., 1991, Geology of the Point Sur–Lopez Point Region, Coast Ranges, California: A Part of the Southern California Allochthon: Geological Society of America Special Paper 266, 23 p., https://doi.org/10.1130/SPE266.

Hall, C.A., and Saleeby, J.B., 2013, Salinia revisited: A crystalline nappe sequence lying above the Nacimiento fault and dispersed along the San Andreas fault system, central California: International Geology Review, v. 55, p. 1575–1615, https://doi.org/10.1080/00206814.2013.825141.

Hansen, E., and Stuk, M., 1993, Orthopyroxene-bearing, mafic migmatites at Cone Peak, California: Evidence for the formation of migmatitic granulites by anatexis in an open system: Journal of Metamorphic Geology, v. 11, p. 291–307, https://doi.org/10.1111/j.1525-1314.1993.tb00148.x.

Hardebeck, J.L., 2010, Seismotectonics and fault structure of the California Central Coast: Bulletin of the Seismological Society of America, v. 100, p. 1031–1050, https://doi.org/10.1785/0120090307.

Jacobson, C.E., Grove, M., Pedrick, J.N., Barth, A.P., Marsaglia, K.M., Gehrels, G.E., and Nourse, J.A., 2011, Late Cretaceous–early Cenozoic tectonic evolution of the southern California margin inferred from provenance of trench and forearc sediments: Geological Society of America Bulletin, v. 123, p. 485–506, https://doi.org/10.1130/B30238.1.

Jennings, C.W., and Bryant, W.A., compilers, 2010, Fault activity map of California: California Geological Survey Geologic Data Map 6, scale 1:750,000.

Johnson, S.Y., Watt, J.T., Hartwell, S.R., and Kluesner, J.W., 2018, Neotectonics of the Big Sur bend, San Gregorio–Hosgri fault system, central California: Tectonics, v. 37, p. 1930–1954, https://doi.org/10.1029/2017TC004724.

Johnston, S.M., Kylander-Clark, A.R.C., and Chapman, A.D., 2018, Detrital zircon geochronology and evolution of the Nacimiento block late Mesozoic forearc basin, central California coast, *in* Ingersoll, R.V., Lawton, T.F., and Graham, S.A., eds., Tectonics, Sedimentary Basins, and Provenance: A Celebration of the Career of William R. Dickinson: Geological Society of America Special Paper 540, p. 383–407, https://doi.org/10.1130.2018.2540(17).

Keppie, J.D., Hynes, A.J., Lee, J.K.W., and Norman, M., 2012, Oligocene-Miocene back-thrusting in southern Mexico linked to the rapid subduction erosion of a large forearc block: Tectonics, v. 31, TC2008, https://doi.org/10.1029/2011TC002976.

Kidder, S., Ducea, M., Gehrels, G., Patchett, P.J., and Vervoort, J., 2003, Tectonics and magmatic development of the Salinian Coast Ridge Belt, California: Tectonics, v. 22, 1058, https://doi.org/10.1029/2002TC001409.

Kistler, R., and Peterman, Z.E., 1978, Reconstruction of crustal blocks of California on the basis of initial strontium isotopic compositions of Mesozoic granitic rocks: U.S. Geological Survey Professional Paper 1071, 17 p., https://doi.org/10.3133/pp1071.

Langenheim, V.E., Jachens, R.C., Graymer, R.W., Colgan, J.P., Wentworth, C.M., and Stanley, R.G., 2013, Fault geometry and cumulative offsets in the central Coast Ranges, California: Evidence for northward increasing slip along the San Gregorio–San Simeon–Hosgri fault: Lithosphere, v. 5, p. 29–48, https://doi.org/10.1130/L233.1.

Lettis, W.R., Hanson, K.L., Unruh, J.R., McLaren, M., and Savage, W.U., 2004, Quaternary tectonic setting of south-central coastal California: U.S. Geological Survey Bulletin 1995-AA, 21 p.

Marrett, R.A., and Allmendinger, R.W., 1990, Kinematic analysis of fault-slip data: Journal of Structural Geology, v. 12, p. 973–986, https://doi.org/10.1016/0191-8141(90)90093-E.

Mattinson, J.M., 1978, Age, origin, and thermal histories of some plutonic rocks from the Salinian block of California: Contributions to Mineralogy and Petrology, v. 67, p. 233–245, https://doi.org/10.1007/BF00381451.

Mattinson, J.M., 1990, Petrogenesis and evolution of the Salinian magmatic arc, *in* Anderson, J.L., ed., The Nature and Origin of Cordilleran Magmatism: Geological Society of America Memoir 174, p. 237–250, https://doi.org/10.1130/MEM174-p237.

McCaffrey, R., Zwick, P.C., Bock, Y., Prawirodirdjo, L., Genrich, J.F., Stevens, C.W., Puntodewo, S.S.O., and Subarya, C., 2000, Strain partitioning during oblique plate convergence in northern Sumatra: Geodetic and seismologic constraints and numerical modeling: Journal of Geophysical Research, v. 105, p. 28,363–28,376, https://doi.org/10.1029/1999JB900362.

McLaren, M.K., and Savage, W.U., 2001, Seismicity of south-central coastal California: October 1987 through January 1997: Bulletin of the Seismological Society of America, v. 91, p. 1629–1658, https://doi.org/10.1785/0119980192.

McLaren, M.K., Hardebeck, J.L., van der Elst, N., Unruh, J.R., Bawden, G.W., and Blair, J.L., 2008, Complex faulting associated with the 22 December 2003 Mw 6.5 San Simeon, California, earthquake, aftershocks, and postseismic surface deformation: Bulletin of the Seismological Society of America, v. 98, p. 1659–1680, https://doi.org/10.1785/0120070088.

McWilliams, M.O., and Howell, D.G., 1982, Exotic terranes of western California: Nature, v. 297, p. 215–217, https://doi.org/10.1038/297215a0.

Moore, J.C., 1978, Orientation of underthrusting during latest Cretaceous and earliest Tertiary time, Kodiak Islands, Alaska: Geology, v. 6, p. 209–213, https://doi.org/10.1130/0091-7613(1978)6<209:OOUDLC>2.0.CO;2.

Naeser, C.W., and Ross, D.C., 1976, Fission-track ages of sphene and apatite of granitic rocks of the Salinian block, Coast Ranges, California: Journal of Research of the U.S. Geological Survey, v. 4, p. 415–420.

Norris, R., 1985, Geology of the Landels-Hill Big Creek Reserve, Monterey County, California: University of California, Santa Cruz, Environmental Field Program Publication 16, 71 p.

Page, B.M., 1970, Sur-Nacimiento fault zone of California: Continental margin tectonics: Geological Society of America Bulletin, v. 81, p. 667–690, https://doi.org/10.1130/0016-7606(1970)81[667:SFZOCC]2.0.CO;2.

Page, B.M., 1972, Oceanic crust and mantle fragment in subduction complex near San Luis Obispo, California: Geological Society of America Bulletin, v. 83, p. 957–972, https://doi.org/10.1130/0016-7606(1972)83[957:OCAMFI]2.0.CO;2.

Page, B.M., 1982, Migration of Salinian composite block, California, and disappearance of fragments: American Journal of Science, v. 282, p. 1694–1734, https://doi.org/10.2475/ajs.282.10.1694.

Pavlis, T.L., and Roeske, S.M., 2007, The Border Ranges fault system, southern Alaska, *in* Ridgway, K.D., Trop, J.M., Glen, J.M.G., and O'Neil, J.M., eds., Tectonic Growth of a Collisional Continental Margin: Crustal Evolution of Southern Alaska: Geological Society of America Special Paper 431, p. 95–127, https://doi.org/10.1130/2007.2431(05).

Reiche, P., 1937, Geology of the Lucia quadrangle, California: Bulletin of the Department of Geological Sciences, University of California, v. 24, p. 115–168.

Ross, D.C., 1976, Reconnaissance geologic map of pre-Cenozoic basement rocks, northern Santa Lucia Range, Monterey County, California: U.S. Geological Survey Miscellaneous Field Studies Map MF-750, https://doi.org/10.3133/mf750.

Ruetz, J.W., 1979, Paleocene submarine fan deposits of the Indians Ranch area, Monterey County, California, *in* Graham, S.A., ed., Tertiary and Quaternary Geology of the Salinas Valley and Santa Lucia Range, Monterey County, California: Society of Economic Paleontologists and Mineralogists, Pacific Section, Pacific Coast Paleogeography Field Guide 4, p. 13–24.

Seiders, V.M., 1983, Correlation and provenance of upper Mesozoic chert-rich conglomerate of California: Geological Society of America Bulletin, v. 94, p. 875–888, https://doi.org/10.1130/0016-7606(1983)94<875:CAPOUM>2.0.CO;2.

Seiders, V.M., Joyce, J.M., Leverett, K.A., and McLean, H., 1983, Geologic map of part of the Ventana Wilderness and the Black Butte, Bear Mountain, and Bear Canyon roadless areas, Monterey County, California: U.S. Geological Survey Miscellaneous Field Studies Map MF-1159-B, https://doi.org/10.3133/mf1559B.

Sharman, G.R., Graham, S.A., Grove, M., and Hourigan, J.K., 2013, A reappraisal of the early slip history of the San Andreas fault, central California, USA: Geology, v. 41, p. 727–730, https://doi.org/10.1130/G34214.1.

Singleton, J.S., and Cloos, M., 2013, Kinematic analysis of mélange fabrics in the Franciscan Complex near San Simeon, California: Evidence for sinistral slip on the Nacimiento fault zone?: Lithosphere, v. 5, p. 179–188, https://doi.org/10.1130/L259.1.

Sorlien, C.C., Kamerling, M.J., and Mayerson, D., 1999, Block rotation and termination of the Hosgri strike-slip fault, California, from a three-dimensional map restoration: Geology, v. 27, p. 1039–1042, https://doi.org/10.1130/0091-7613(1999)027<1039:BRATOT>2.3.CO;2.

Tapponnier, P., Peltzer, G., Le Dain, A.Y., Armijo, R., and Cobbold, P., 1982, Propagating extrusion tectonics in Asia: New insight from simple experiments with plasticine: Geology, v. 10, p. 611–616, https://doi.org/10.1130/0091-7613(1982)10<611:PETIAN>2.0.CO;2.

Titus, S.J., Dyson, M., DeMets, C., Tikoff, B., Rolandone, F., and Bürgmann, R., 2011, Geologic versus geodetic deformation adjacent to the San Andreas fault, central California: Geological Society of America Bulletin, v. 123, p. 794–820, https://doi.org/10.1130/B30150.1.

Trasko, K.P., and Cloos, M., 2007, Faulting in the Lopez Point–Ragged Point segment of Highway 1, southern Big Sur area, California: Implications for the Nacimiento fault: Geological Society of America, Abstracts with Programs, v. 39, no. 4, p. 52.

Ukar, E., 2012, Tectonic significance of low-temperature blueschist blocks in the Franciscan mélange at San Simeon, California: Tectonophysics, v. 568–569, p. 154–169, https://doi.org/10.1016/j.tecto.2011.12.039.

Underwood, M.B., Laughland, M.M., Shelton, K.L., and Sedlock, R.L., 1995, Thermal-maturity trends within Franciscan rocks near Big Sur, California: Implications for offset along the San Gregorio–San Simeon–Hosgri fault zone: Geology, v. 23, p. 839–842, https://doi.org/10.1130/0091-7613(1995)023<0839:TMTWFR>2.3.CO;2.

Vedder, J.G., Howell, D.G., and McLean, H., 1983, Stratigraphy, sedimentation, and tectonic accretion of exotic terranes, southern Coast Ranges, California, *in* Howell, D.G., Vedder, J.G., and McDougall, K., eds., Cretaceous Geology of the California Coast Ranges, West of the San Andreas Fault: Society of Economic Paleontologists and Mineralogists, Pacific Section, Pacific Coast Paleogeographic Field Guide 2, p. 71–78.

Vedder, J.G., McLean, H., Stanley, R.G., and Wiley, T.J., 1991, Paleogeographic implications of an erosional remnant of Paleogene rocks southwest of the Sur-Nacimiento fault zone, southern Coast Ranges, California: Geological Society of America Bulletin, v. 103, p. 941–952, https://doi.org/10.1130/0016-7606(1991)103<0941:PIOAER>2.3.CO;2.

von Huene, R., and Scholl, D.W., 1991, Observations at convergent margins concerning sediment subduction, subduction erosion, and the growth of continental crust: Reviews of Geophysics, v. 29, p. 279–316, https://doi.org/10.1029/91RG00969.

Willis, C.J., Manson, M.W., Brown, K.D., Davenport, C.W., and Domrose, C.J., 2001, Landslides in the Highway 1 corridor: Geology and slope stability along the Big Sur coast between Point Lobos and San Carpoforo Creek, Monterey and San Luis Obispo Counties, California: California Geological Survey Special Report 185, 40 p.

Wyld, S.J., Umhoefer, P.J., and Wright, J.E., 2006, Reconstructing northern Cordilleran terranes along known Cretaceous and Cenozoic strike-slip faults: Implications for the Baja British Columbia hypothesis and other models, *in* Haggart, J.W., Enkin, R.J., and Monger, J.W.H., eds., Paleogeography of the North American Cordillera: Evidence For and Against Large-Scale Displacements: Geological Association of Canada Special Paper 46, p. 277–298.